Unknown input observer in descriptor form via LMIs for power-assisted wheelchairs

Guoxi Feng[1], Thierry Marie Guerra[1], Lucian Busoniu[2], Sami Mohammad[3]

1. *LAMIH, UMR CNRS 8530, University of valenciennes Le Mont Houy, 59313 Valenciennes Cedex 9, France*
E-Mail: {guoxi.feng, guerra}@univ-valenciennes.fr
2. *Department of Automation, Technical University of Cluj-Napoca, Memorandumului 28, 400114 Cluj-Napoca, Romania*
E-mail: lucian@busoniu.net
3. *AutoNomad Mobility, Le Mont Houy 59313 Valenciennes Cedex 9, France*
E-mail: sami.mohammad@autonomad-mobility.com

Abstract: Power-assisted wheelchairs (PAW) provide an efficient means of transport for disabled persons. In this human-machine interaction, the human-applied torque is a crucial variable to implement the assistive system. The present paper describes a novel scheme to design PAWs without torque sensors. Instead of using a torque sensor, a discrete-time unknown input observer in descriptor form is applied to estimate the human input torque and the angular velocities of the two wheels via the angular position. Using Finsler's lemma, the observer gains are obtained by solving an LMI problem. Based on the estimation, both a torque-assistance system and a speed controller are introduced. In addition, the Input-to-State Stability (ISS) of the interconnected controller-observer system is analysed for the speed controller. Finally, simulation results validate the observer and the power-assisted algorithms. The methodology follows patent WO2015173094 issued in 2015 [20].

Keywords: Disabled person, power-assisted wheelchair, descriptor model, linear matrix inequality (LMI), Lyapunov function, unknown input observer (UIO).

1. Introduction

According to the World Health Organization (WHO), disabled people and elderly persons who lose the ability to walk occupy a significant percentage of the population in ageing societies [26]. The manual wheelchair is a common means to improve accessibility and mobility for such disabled persons. However, the majority of them have difficulty to propel a manual wheelchair effectively due to the body's constraints or unpredictable road conditions [5]. This poor efficiency of manual wheelchairs can cause secondary injuries to the users (e.g. joint degradation) [8]. Of course, a solution is the traditional electric wheelchair [15], [17] that provides all the necessary energy. Nevertheless, this solution implies a complete stop of physical activities of the disabled persons which is definitively not recommended by specialists [16]. An intermediate solution, the power-assisted wheelchairs (PAW), can provide an alternative means to wheelchair users. Having an electrically powered motor, PAWs supplement the manual push to reduce the user's physical workloads. In contrast with manual wheelchairs and fully automatic wheelchairs, PAW combines human and electrical power and therefore gives a good compromise between rest and exercise for users. Several PAWs are available amongst which the motorisation kits Duo and Nomad designed by AutoNomad Mobility [20]. These kits can be installed on most manual wheelchairs and offer good manoeuvrability. The medical investigations [18], [19] show the physical and physiological advantages derived from the PAW rather than fully manual or automatic solutions (e.g. moderate metabolic demands of propulsion, maintaining participation in community-based activities).

There is a rapidly growing literature on PAW designs. References [1]-[4] have analysed the impact of different road conditions on the human-wheelchair system. A corresponding control scheme has been implemented to assist the user for each road condition. In [9] the human behaviour and the interaction with the device are studied. The experimental results of the clinical studies [6], [7] have shown clearly the assisted mechanical efficiency given by the PAW to the user.

In classical PAWs, the torque exerted on the hand-rims is an important signal to design the control law. Generally, this signal is measured directly by a torque sensor. More recently, many works apply different sensors to estimate the disabled person's intention and the condition of the road [10], [11]. Based on these estimations or measurements, power-assisted algorithms can be implemented to help the users. However, due to the high cost of sensors, current experimental or commercial PAWs are often not affordable to disabled persons. This issue is compelling reason to design software sensors for PAWs [20].

The present study relies on patent WO2015173094 issued in 2015 [20]. In the present paper, we focus on the input torque estimation problem. The unknown input torques exerted on the wheelchair are estimated by using a so-called unknown input observer (UIO) approach [29], [28], which is widely used in fault diagnosis, fault-tolerant control and disturbance estimation. In the similar work [12], a torque observer is designed based on two velocity sensors. Compared to [12], we estimate the unknown input torque using the signal of wheel angular positions measured by inexpensive encoders. In addition, a structure of the observer using a descriptor form model [21]-[23] is applied to obtain LMI conditions [27]. A proportional power-assistance systems and a PI velocity controller based on the estimated signals are proposed. Moreover, numerical simulations show the efficacy of our torque-sensorless PAW design.

This paper is organized as follows. In Section 2, we introduce the mathematical model of the wheelchair. Section 3 elaborates the unknown input observer in descriptor form to estimate the input torques and the angular velocities of two wheels. Section 4 provides two power-assisted algorithms and the complete proof of closed-loop stability. In Section 5,

simulation results validate the proposed observer and algorithms. Section 6 gives our conclusions.

2. Wheelchair Modelling

In this study, the wheelchair is modelled as a two wheeled transporter. We consider that the caster's dynamics can be neglected. Fig. 1 shows the two dimensional schematic of the wheelchair, where θ_L and θ_R are respectively the left angular position and the right angular position, r is the wheel radius, d is the distance between two wheels and c is the centre of gravity of the wheelchair with the human.

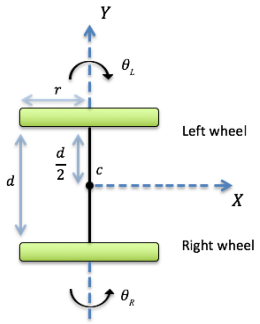

Figure 1: Simplified top view of the wheelchair

By solving the Lagrange equation [13]-[15], the two-wheeled PAW can be described by the dynamics:

$$\begin{aligned} \alpha\ddot{\theta}_R + \beta\ddot{\theta}_L &= T_R - K\dot{\theta}_R \\ \alpha\ddot{\theta}_L + \beta\ddot{\theta}_R &= T_L - K\dot{\theta}_L \end{aligned} \tag{1}$$

where the inertial parameters α and β are:

$$\begin{aligned} \alpha &= \frac{mr^2}{4} + \frac{I_C r^2}{b^2} + I_0 \\ \beta &= \frac{mr^2}{4} - \frac{I_C r^2}{b^2} \end{aligned} \tag{2}$$

Here, m denotes the mass of wheelchair including the human, K represents the viscous friction coefficient, I_C is the inertia of the wheelchair with respect to the vertical axis through c, I_0 is the inertia of each driving wheel around the wheel axis, and finally T_R and T_L are the total torques exerted on the right wheel and the left wheel respectively. It is assumed that the driving road is flat. The total torques consists of the unknown torques T_{Rh}, T_{Lh} exerted by user and the assistive torques T_{Rm}, T_{Lm} given by the electrical motors:

$$\begin{aligned} T_R &= T_{Rh} + T_{Rm} \\ T_L &= T_{Lh} + T_{Lm} \end{aligned} \tag{3}$$

From the dynamic equations (1) and the inertial parameters (2), the wheelchair's behaviour is strongly linked to the mass of user and the conditions of road.

Descriptor form models are widely employed to describe mechanical systems, and they provide important advantages for controller/observer design such as reducing the number of linear models and LMI constraints for Takagi-Sugeno models [21]-[23]. By choosing the state vector $x^T = [\theta_R, \theta_L, \dot{\theta}_R, \dot{\theta}_L]$, the unknown inputs $u_h^T = [T_{Rh}, T_{Lh}]$, the known inputs $u_m^T = [T_{Rm}, T_{Lm}]$ and the outputs $y^T = [\theta_R, \theta_L]$, the mechanical system (1) can be rewritten in the following descriptor form:

$$\begin{aligned} E\dot{x}(t) &= Ax(t) + Bu_h(t) + Bu_m(t) \\ y(t) &= Cx(t) \end{aligned} \tag{4}$$

where the matrices are:

$$E = \begin{bmatrix} 1 & 0 & 0 & 0 \\ 0 & 1 & 0 & 0 \\ 0 & 0 & \alpha & \beta \\ 0 & 0 & \beta & \alpha \end{bmatrix}, A = \begin{bmatrix} 0 & 0 & 1 & 0 \\ 0 & 0 & 0 & 1 \\ 0 & 0 & -K & 0 \\ 0 & 0 & 0 & -K \end{bmatrix},$$
$$B = \begin{bmatrix} 0 & 0 \\ 0 & 0 \\ 1 & 0 \\ 0 & 1 \end{bmatrix}, C = \begin{bmatrix} 1 & 0 & 0 & 0 \\ 0 & 1 & 0 & 0 \end{bmatrix}.$$

Remark 1. In the descriptor system (4), all the inertial parameters are on the left hand-side of the equation. Compared to the conventional state-space form, the descriptor form preserves the physical interpretation of mechanical systems. Due to the "natural" descriptor form of the mechanical system (1), this form is kept for the reminder of the paper.

3. Unknown Input Estimation

In this section, an LMI-based design procedure is presented for the unknown input observer in descriptor form. The state and the unknown input torque are estimated simultaneously by the proposed observer. Through a Lyapunov function and Finsler's lemma, the observer gains are found from an LMI feasible solution. The following lemma will be used:

Lemma 1. [24] (Finsler's lemma). Let $X \epsilon \mathbb{R}^n$, $Q = Q^T \epsilon \mathbb{R}^{n \times n}$, and $W \epsilon \mathbb{R}^{m \times n}$ such that $\text{rank}(W) < n$; the following expressions are equivalent:

a) $X^Y Q X < 0, \forall X \epsilon \{ X \epsilon \mathbb{R}^n : X \neq 0, WX = 0 \}$

b) $\exists M \epsilon \mathbb{R}^{n \times m} : MW + W^T M^T + Q < 0$

3.1. Discrete-time Descriptor System

To derive a discrete-time model, the classical Euler's method has been used with $\dot{x}(t) = (x(k+1) - x(k))/s$, where s is the sampling time. Then, the discrete time model in descriptor form is:

$$\begin{aligned} E_d x(k+1) &= A_d(k) + B_d u_h(k) + B_d u_m(k) \\ y(k) &= Cx(k) \end{aligned} \tag{5}$$

with the following matrices:

$$E_d = \begin{bmatrix} 1 & 0 & 0 & 0 \\ 0 & 1 & 0 & 0 \\ 0 & 0 & \alpha & \beta \\ 0 & 0 & \beta & \alpha \end{bmatrix}, A_d = \begin{bmatrix} 1 & 0 & s & 0 \\ 0 & 1 & 0 & s \\ 0 & 0 & \alpha - sK & \beta \\ 0 & 0 & \beta & \alpha - sK \end{bmatrix},$$
$$B_d = (B_{d1} \quad B_{d2}) = \begin{bmatrix} 0 & 0 \\ 0 & 0 \\ s & 0 \\ 0 & s \end{bmatrix}, C_d = \begin{bmatrix} 1 & 0 & 0 & 0 \\ 0 & 1 & 0 & 0 \end{bmatrix}.$$

3.2. Polynomial Approximation Approach

We consider that the unknown input torques T_{Rh} and T_{Lh} exerted on the wheels can be approximated by a n_pth degree polynomial function in time, for example for the right wheel $d^{n_p} T_{Rh}/dt^{n_p} = 0$. Using this assumption, the discrete-time input torques can be expressed as:

$$(1 - z^{-1})^{n_p} T_{Rh}(k) = 0 \tag{6}$$

Further, (6) can be expressed as:

$$T_{Rh}(k) = -\sum_{i=1}^{n_p} \binom{n_p}{i} (-1)^{n_p} T_{Rh}(k-i) \tag{7}$$

where $\binom{n_p}{i}$ is the binomial coefficient. Consider the unknown input vector $T_{Rh}^{n_p}(k) = [T_{Rh}(k), T_{Rh}(k-1), \dots, T_{Rh}(k-n_p+1)]^T \epsilon \mathbb{R}^{n_p}$. The dynamics (7) of the vector $T_{Rh}^{n_p}$ can be written as:

$$T_{Rh}^{n_p}(k+1) = \Gamma_{n_P} T_{Rh}^{n_p}(k) \tag{8}$$

where:

$$\Gamma_{n_P} = \begin{bmatrix} -(-1)^1\binom{n_p}{1} & -(-1)^2\binom{n_p}{2} & \dots & -(-1)^{n_p}\binom{n_p}{n_p} \\ I_{n_p-1} & & 0_{(n_p-1)\times 1} & \end{bmatrix}$$

Applying the same reasoning for the left wheel, the dynamics of the vector $T_{Lh}^{n_p}(k) = \left[T_{Lh}(k), T_{Lh}(k-1), \dots, T_{Lh}\left(k-n_p+1\right)\right]^T \epsilon \mathbb{R}^{n_p}$ are:

$$T_{Lh}^{n_p}(k+1) = \Gamma_{n_P} T_{Lh}^{n_p}(k) \tag{9}$$

Defining an extended state vector as $\bar{x} = \left[\theta_R, \theta_L, \dot{\theta}_R, \dot{\theta}_L, T_{Rh}^{n_p T}, T_{Lh}^{n_p T}\right]^T \epsilon \mathbb{R}^{2n_p+4}$, the discrete-time descriptor system (5) can be rewritten as:

$$\begin{aligned} \bar{E}\bar{x}(k+1) &= \bar{A}\bar{x}(k) + B_d u_m(k) \\ y(k) &= \bar{C}\bar{x}(k) \end{aligned} \tag{10}$$

where:

$$\bar{E} = \begin{bmatrix} E_d & 0_{4\times 2n_p} \\ 0_{2n_p\times 4} & I_{2n_p} \end{bmatrix}, \bar{C} = \begin{bmatrix} 1 & 0 & 0 & 0 \\ 0 & 1 & 0 & 0 \end{bmatrix},$$
$$\bar{A} = \begin{bmatrix} A_d & B_{d1} & 0_{4\times(n_p-1)} & B_{d2} & 0_{4\times(n_p-1)} \\ 0_{n_p\times 4} & \Gamma_{n_P} & & 0_{n_p\times n_p} & \\ 0_{n_p\times 4} & 0_{n_p\times n_p} & & \Gamma_{n_P} & \end{bmatrix}.$$

Note that the problem is well posed as $\bar{E}$ is always invertible.

3.3. Observer Design

The aim is to estimate the unknown input torques T_{Rh}, T_{Lh} and the angular velocities $\dot{\theta}_R, \dot{\theta}_L$ from the right and left angular position signals. The observer considered for the descriptor model (10) is:

$$\begin{aligned} \bar{E}\hat{\bar{x}}(k+1) &= \bar{A}\hat{\bar{x}}(k) + B_d u_m(k) + G^{-1}L(y(k) \\ &\quad - \hat{y}(k)) \\ \hat{y}(k) &= \bar{C}\hat{\bar{x}}(k) \end{aligned} \tag{11}$$

The estimation error is $e(k) = \bar{x}(k) - \hat{\bar{x}}(k)$. Its dynamic is given by:

$$\bar{E}e(k+1) = (\bar{A} - G^{-1}L\bar{C})e(k) \tag{12}$$

In order for the estimated states to converge to the real states, the estimation error (12) should be asymptotically stable. Two matrices G and L have to be found to construct the observer (11). Consider the following Lyapunov function candidate:

$$V\left(e(k)\right) = e^T(k)Pe(k) \tag{13}$$

The symmetric matrix $P\epsilon\mathbb{R}^{(2n_p+4)(2n_p+4)}$ is positive-definite, so $P = P^T > 0$. Now we present our main result.

Theorem 1. The estimation error dynamic (12) is asymptotically stable if there exist P, G, L and a scalar decay rate δ with $0 < \delta \leq 1$ such that

$$\begin{bmatrix} -\delta P & * \\ G\bar{A} - L\bar{C} & P - G\bar{E} - \bar{E}^T G^T \end{bmatrix} < 0 \tag{14}$$

Proof. The variation $\Delta V\left(e(k)\right) = V\left(e(k+1)\right) - \delta V(e(k))$ of the Lyapunov function (13) including the decay rate δ is:

$$\Delta V\left(e(k)\right) = \begin{bmatrix} e(k) \\ e(k+1) \end{bmatrix}^T \begin{bmatrix} -\delta P & 0 \\ 0 & P \end{bmatrix} \begin{bmatrix} e(k) \\ e(k+1) \end{bmatrix} < 0 \tag{15}$$

The estimation error dynamics (12) can be rewritten as:

$$\begin{bmatrix} \bar{A} - G^{-1}L\bar{C} & -\bar{E} \end{bmatrix} \begin{bmatrix} e(k) \\ e(k+1) \end{bmatrix} = 0 \tag{16}$$

From Lemma 1, the inequality (15) under constraint (16) is equivalent to solving the following linear matrix inequality:

$$M\begin{bmatrix} \bar{A} - G^{-1}L\bar{C} & -\bar{E} \end{bmatrix} + (*) + \begin{bmatrix} -\delta P & 0 \\ 0 & P \end{bmatrix} < 0 \tag{17}$$

The asterisk $(*)$ represents the transpose of the matrix $M\begin{bmatrix} \bar{A} - G^{-1}L\bar{C} & -\bar{E} \end{bmatrix}$. By choosing $M = [0\ G^T]^T$, we obtain directly the linear matrix inequality (14). ■

Remark 2. Applying the observer gain obtained by solving (14), the Lyapunov function candidate (13) is decreased exponentially as follows:

$$V_{k+1} < \delta V_k < \delta^2 V_{k-1} \cdots < \delta^{k+1} V_0 \tag{18}$$

In this way, the convergence of the estimation error $e(k)$ can be tuned via the decay rate δ.

4. Power-Assisted System

In the previous section, using an unknown input observer, the unknown input torques exerted on the wheelchair and the angular velocities of two wheels can be estimated via the angular position measurements. Next, based on the rebuilt signals, two power-assistance algorithms are designed.

4.1. Proportional Torque-Assistance System Design

The block diagram of the first algorithm is shown in Fig. 2.

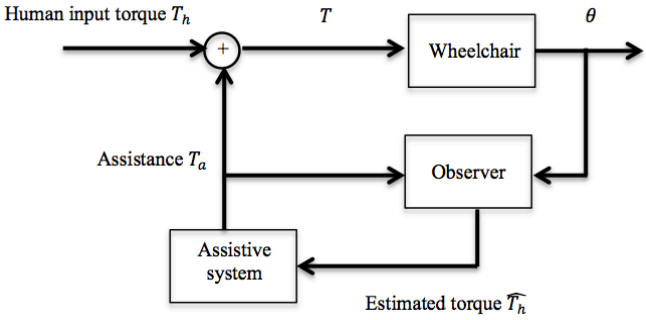

Figure 2: Proportional power-assistance algorithm

The control algorithm above uses an open-loop controller. The assistive torque T_a is generated based on the estimated input torque $\hat{T}_h$. The following discrete-time transfer function describes the dynamics of T_a:

$$T_a(z) = \frac{\psi}{z - e^{-\frac{s}{\tau}}}\hat{T}_h(z) \tag{19}$$

where s is the sample time, ψ is the assistance ratio and τ is the response time parameter of the assistive system. This torque control based system is also known as Low-Pass-Filter proposed in [1]. The assistance ratio ψ determines the total assistive torque and the response time parameter τ determines the inertial dynamics of the assistive torque. These two parameters should be configured correctly to have a good compromise between smooth driving and efficient torque assistance for PAW. The objective is to generate a desired assistive toque to compensate for driving torque shortages. Different parameter setting strategies can be found in [1], [4], e.g, adaptive driving control using parameter adjustment. In the present study, only constant parameters are used to validate our torque-sensorless PAW design.

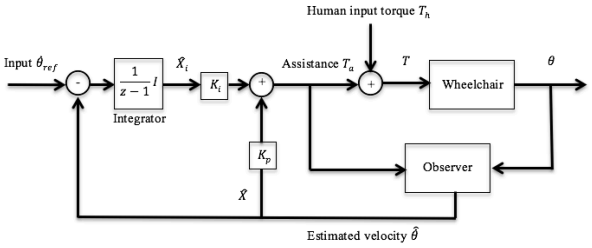

Figure 3: Power assistance algorithm with PI velocity controller and velocity observer

4.2. Observer-based PI Controller Design

A PI controller is added to track a reference velocity as depicted in Fig. 3. We apply the observer (11) rewritten as:

$$E_d\hat{x}(k+1) = A_d\hat{x}(k) + B_d u_m(k) + B_d\hat{u}_h(k) + L_1(y(k) - C_d\hat{x}(k)) \quad (20)$$

$$\begin{bmatrix}\hat{T}_{Rh}^{n_p}(k+1)\\ \hat{T}_{Lh}^{n_p}(k+1)\end{bmatrix} = \begin{bmatrix}\Gamma_{n_p} & 0_{n_p\times n_p}\\ 0_{n_p\times n_p} & \Gamma_{n_p}\end{bmatrix}\begin{bmatrix}\hat{T}_{Rh}^{n_p}(k)\\ \hat{T}_{Lh}^{n_p}(k)\end{bmatrix} + L_2(y(k) - C_d\hat{x}(k)) \quad (21)$$

with $G^{-1}L = [L_1^T \quad L_2^T]^T$, $L_1\epsilon\mathbb{R}^{4\times 2}$, $L_2\epsilon\mathbb{R}^{2n_p\times 2}$ and the estimated unknown inputs $\hat{u}_h^T = [\hat{T}_{Rh}, \hat{T}_{Lh}]$. The proposed PI observer-based controller is:

$$u_m(k) = [K_P \quad K_i]\begin{bmatrix}\hat{X}(k)\\ \hat{X}_i(k)\end{bmatrix} \quad (22)$$

$$\hat{X}(k) = X(k) - e_{\dot{\theta}}(k)$$

$$\hat{X}_i(k+1) - \hat{X}_i(k) = \dot{\theta}_{ref} - X(k) + e_{\dot{\theta}}(k)$$

with the real velocity vector $X = [\dot{\theta}_R \quad \dot{\theta}_L]^T$ and the estimated velocity vector $\hat{X} = \left[\hat{\dot{\theta}}_R \quad \hat{\dot{\theta}}_L\right]^T$. Here $\dot{\theta}_{ref}, e_{\dot{\theta}}$ are the reference velocity and the velocity estimation errors respectively. By defining the angular position estimation errors e_θ, the state vector $X^* = \left[X \quad \hat{X}_i \quad e_\theta \quad e_{\dot{\theta}}\right]^T$, the unknown input estimation errors $\varepsilon_T = u_h - \hat{u}_h$, and $U^* = \left[u_h \quad \dot{\theta}_{ref} \quad \varepsilon_T\right]^T$, the closed-loop dynamics are:

$$E_d^*X^*(k+1) = A_d^*X^*(k) + B_d^*U^*(k) \quad (23)$$

with the following matrices:

$$E_d^* = \begin{bmatrix}\alpha & \beta & 0_{2\times 6}\\ \beta & \alpha & \\ 0_{6\times 2} & & I_6\end{bmatrix}, A_d^* = \begin{bmatrix}A_{\dot{\theta}} + B_{\dot{\theta}}K_P & B_{\dot{\theta}}K_i & 0_{2\times 2} & -K_P\\ -I_2 & I_2 & 0_{2\times 2} & I_2\\ 0_{4\times 4} & & A_d - L_1C_d & \end{bmatrix},$$

$$B_d^* = \begin{bmatrix}0_{4\times 2} & 0_{4\times 2} & B_d\\ B_{\dot{\theta}} & 0_{2\times 2} & 0_{2\times 2}\\ 0_{2\times 2} & I_2 & 0_{2\times 2}\end{bmatrix}, A_{\dot{\theta}} = \begin{bmatrix}\alpha - sK & \beta\\ \beta & \alpha - sK\end{bmatrix}, B_{\dot{\theta}} = \begin{bmatrix}s & 0\\ 0 & s\end{bmatrix}.$$

Assume that the unknown input u_h, the unknown input estimation errors ε_T, and the reference velocity $\dot{\theta}_{ref}$ are bounded ($U^* \in L_\infty$). These "natural" assumptions will allow deriving an Input-to-State property (ISS) for the closed-loop system (23).

Lemma 2. [25] Consider a Lyapunov function candidate $V: \mathbb{R}^n \to \mathbb{R}^+$, $V(0) = 0$ and $V(x) > 0$ $(x \neq 0)$ for a general discrete system $x(k+1) = f(x(k), u(k))$. If there exist $\mathcal{K}_\infty$-function γ and $\mathcal{K}$-function σ such that

$$V(k) = V(k+1) - V(k) \leq \sigma(\|u\|) - \gamma(\|x\|) \quad (24)$$

then the discrete system $x(k+1) = f(x(k), u(k))$ is input-to-state stable.

Proposition 1. Assume that the real velocity vector $X(k) = [\dot{\theta}_R \quad \dot{\theta}_L]^T$ is accessible to the PI controller (22) and the inputs U^* are bounded. Applying velocity feedback control, the closed-loop dynamics are:

$$\begin{bmatrix}\alpha & \beta & 0_{2\times 2}\\ \beta & \alpha & \\ 0_{2\times 2} & & I_2\end{bmatrix}\begin{bmatrix}X(k+1)\\ X_i(k+1)\end{bmatrix} = \begin{bmatrix}A_{\dot{\theta}} + B_{\dot{\theta}}K_P & B_{\dot{\theta}}K_i\\ -I_2 & I_2\end{bmatrix}\begin{bmatrix}X(k)\\ X_i(k)\end{bmatrix} + \begin{bmatrix}B_{\dot{\theta}}\\ 0_{2\times 2}\end{bmatrix}u_h + \begin{bmatrix}0_{2\times 2}\\ I_2\end{bmatrix}\dot{\theta}_{ref} \quad (25)$$

where $X_i(k+1) - X_i(k) = \dot{\theta}_{ref} - X(k)$. Design the controller gains $[K_P \quad K_i]$ through pole placement of the system (25) in interior of the unit circle in the z-plane. Then the closed-loop dynamic (23) is ISS for $U^* \in L_\infty$ (U^* as input and X^* as state).

Proof. Since the matrix A_d^* is block-triangular and the descriptor matrix E_d^* is block-diagonal, the eigenvalues of (23) are those of the closed-loop dynamic (25) and the observer (20) chosen previously by Proposition 1 and Theorem 1 respectively. Thus the closed-loop system (23) is globally asymptotically stable with $U^* = 0$. When $U^* \neq 0$, we consider the Lyapunov function candidate (with symmetric matrix $P^* > 0$):

$$V^*(X^*(k)) = X^{*T}(k)P^*X^*(k) \quad (26)$$

Its variation $\Delta V^*(X^*(k)) = V(X^*(k+1)) - V(X^*(k))$ gives:

$$\Delta V^*(k) = X^{*T}(k)A_d^{T}E_d^{-T}P^*E_d^{-1}A_dX^*(k) + 2X^{*T}(k)A_d^{T}E_d^{-T}P^*E_d^{-1}B_dU^*(k) + U^{*T}(k)B_d^{T}E_d^{-T}P^*E_d^{-1}B_dU^*(k) - X^{*T}(k)P^*X^*(k) \quad (27)$$

There exists positive constant λ such that:

$$\Delta V^*(k) \leq -\lambda\|X^*(k)\|^2 + 2X^{*T}(k)A_d^{T}E_d^{-T}P^*E_d^{-1}B_dU^*(k) + U^{*T}(k)B_d^{T}E_d^{-T}P^*E_d^{-1}B_dU^*(k) \quad (28)$$

Applying norm properties:

$$\Delta V^*(k) \leq -\lambda\|X^*(k)\|^2 + 2\|X^*(k)\|\|A_d^{T}E_d^{-T}P^*E_d^{-1}B_d\|\|U^*(k)\| + \|B_d^{T}E_d^{-T}P^*E_d^{-1}B_d\|\|U^*(k)\|^2 \quad (29)$$

There exist positive constants ϑ and ρ such that:

$$\Delta V^*(k) \leq -\frac{\lambda}{2}\|X^*(k)\|^2 - \left(\sqrt{\frac{\lambda}{2}}\|X^*(k)\| - \vartheta\sqrt{\frac{2}{\lambda}}\|U^*(k)\|\right)^2 + \left(\frac{2\vartheta^2}{\lambda} + \rho\right)\|U^*(k)\|^2 \quad (30)$$

We obtain finally:

$$\Delta V^*(k) \leq -\frac{\lambda}{2}\|X^*(k)\|^2 + \left(\frac{2\vartheta^2}{\lambda} + \rho\right)\|U^*(k)\|^2 \quad (31)$$

Through Lemma 2, the closed-loop system (23) is ISS. ■

Remark 3. In practice, the angular velocities are not measured directly. They are estimated from the position signals. From a methodological point of view, the interest of Proposition 1 is that the estimated signal can be used as the real signals to realize a control policy.

Remark 4. The result in Proposition 1 states that if the inputs U^* are bounded, the states X^* are bounded. Moreover, the controller (22) and the unknown input observer (11) can

be designed separately, and the global stability of the closed-loop system (23) is still guaranteed.

5. Simulation Results

In order to carry out the numerical simulations, we choose the sampling time $s = 0.05sec$ and the following wheelchair parameters: $m = 150kg$, $I_C = 40kg.m^2$, $I_0 = 0.25kg.m^2$, $b = 0.6m$, $r = 0.33m$ and $K = 10N.m.s$. Regarding the observer structure, a 4th degree polynomial is applied for the approximating function (7).

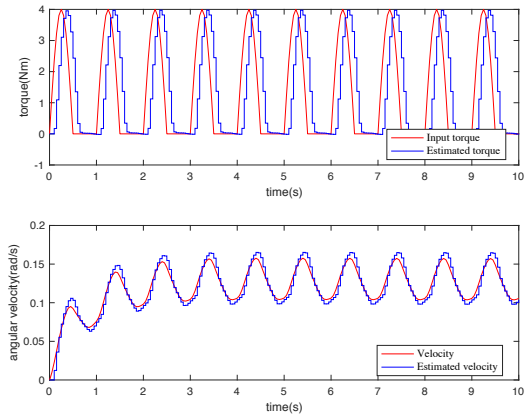

Figure 4: Driving simulation on a flat road without assistance (torque/velocity)

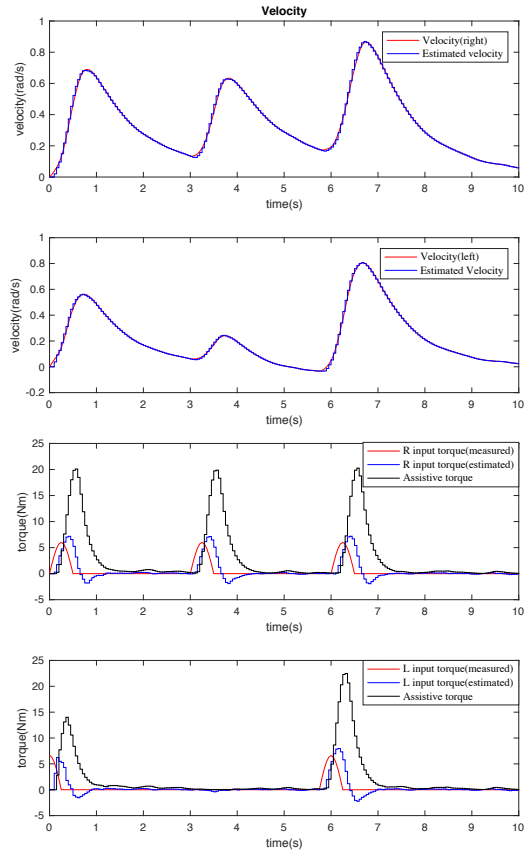

Figure 5: Driving simulation on a flat road with the proposed proportional power-assistance system (1st-trial)

5.1. UIO without power-assistance

The PAW is assumed to move on a flat surface and the human input torque is represented by the positive half cycle of a sinusoidal. The human input torque and the angular velocity are successfully rebuilt, see Fig. 4. Note that there is a delay (two sampling time units) induced by the observer between the real input torque signal and the estimated one.

5.2. UIO with power-assistance

In this section, a power-assisted system is added to help the user to propel the wheelchair on a flat road. The objective is to apply different input torques to check the performance of the proposed observer under two proposed power-assisted algorithms. A Gaussian white noise is added to the inputs to simulate small road irregularities. On the first trial, the assistive torque is generated by (19). As depicted in Fig. 5, the assistive torques are amplified with respect to the estimated torques rebuilt by the observer (11). The estimated torques are slightly deformed due to the delay induced by the observer.

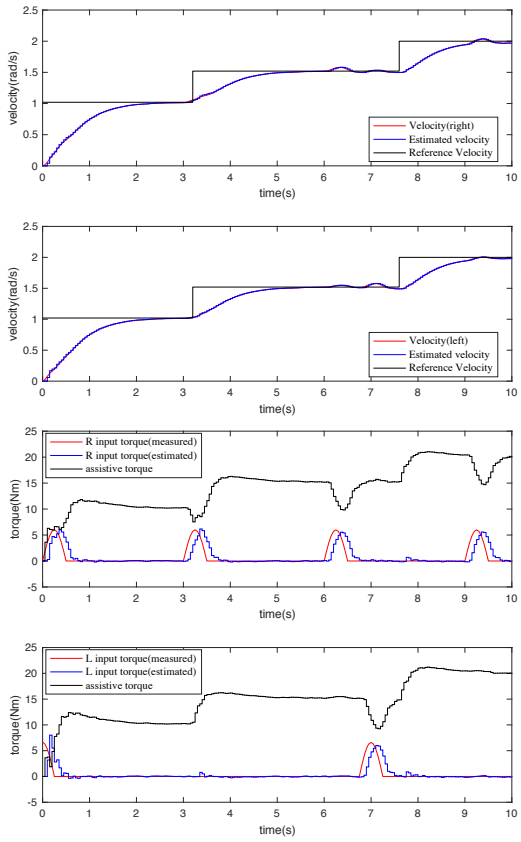

Figure 6: Driving simulation on a flat road with the proposed PI velocity controller (2nd-trial)

For the second and third trial, the proposed PI controller (22) is applied to track a reference velocity with different human input frequencies. The applied input on the 3rd trial have a higher frequency than that used on the 2nd trial. Both Fig. 6 and 7 illustrate that the proposed observer tracks well the state of the wheelchair and the unknown input torques despite the small road irregularities. Moreover, the velocity tracking objectives have been met. The delay induced by the observer dynamic implies that for each sudden change in assistive torques a small spike appears in estimated signals.

6. Conclusion

In this paper, an unknown input observer has been designed to estimate human input torques and angular velocities in

PAW. Based on the proposed observer, two power-assisted algorithms have been implemented to assist users in pushing

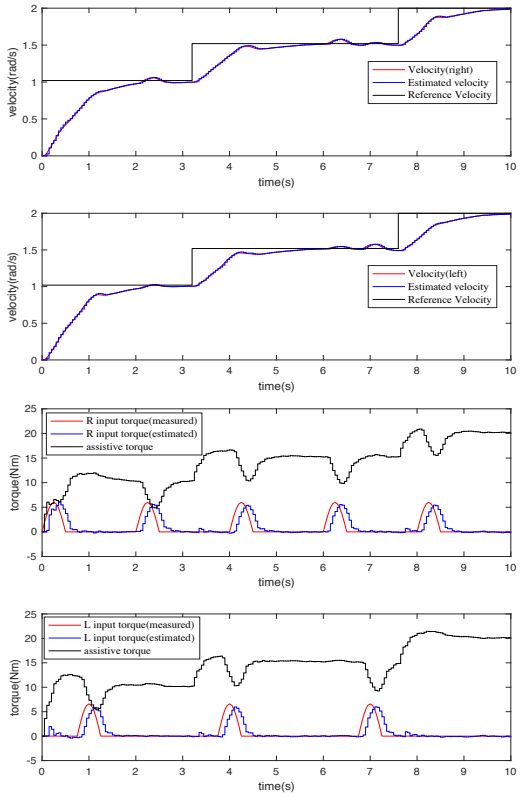

Figure 7: Driving simulation on a flat road with the proposed PI velocity controller (3rd-trial)

the wheelchair and to reduce their excessive physical exertion. The main advantage of these approaches is that input torque signals can be obtained without using torque sensors. This torque-sensorless design can significantly reduce hardware complexity and system cost [20].

References

[1] Seki, H., & Kiso, A. (2011, August). Disturbance road adaptive driving control of power-assisted wheelchair using fuzzy inference. In 2011 Annual International Conference of the IEEE Engineering in Medicine and Biology Society (pp. 1594-1599). IEEE.

[2] Seki, H., Ishihara, K., & Tadakuma, S. (2009). Novel regenerative braking control of electric power-assisted wheelchair for safety downhill road driving. IEEE Transactions on Industrial Electronics, 56(5), 1393-1400.

[3] Seki, H., Sugimoto, T., & Tadakuma, S. (2005, October). Novel straight road driving control of power assisted wheelchair based on disturbance estimation and minimum jerk control. In Fourtieth IAS Annual Meeting. Conference Record of the 2005 Industry Applications Conference, 2005. (Vol. 3, pp. 1711-1717). IEEE.

[4] Seki, H., & Tadakuma, S. (2006, November). Straight and circular road driving control for power assisted wheelchair based on fuzzy algorithm. In IECON 2006-32nd Annual Conference on IEEE Industrial Electronics (pp. 3898-3903). IEEE.

[5] Cooper, R. A., Fitzgerald, S. G., Boninger, M. L., Prins, K., Rentschler, A. J., Arva, J., & O'Connor, T. J. (2001). Evaluation of a pushrim-activated, power-assisted wheelchair. Archives of Physical Medicine and Rehabilitation, 82(5), 702-708.

[6] Arva, J., Fitzgerald, S. G., Cooper, R. A., & Boninger, M. L. (2001). Mechanical efficiency and user power requirement with a pushrim activated power assisted wheelchair. Medical Engineering & Physics, 23(10), 699-705.

[7] Giacobbi Jr, P. R., Levy, C. E., Dietrich, F. D., Winkler, S. H., Tillman, M. D., & Chow, J. W. (2010). Wheelchair users' perceptions of and experiences with power assist wheels. American Journal of Physical Medicine & Rehabilitation, 89(3), 225-234.

[8] Algood, S. D., Cooper, R. A., Fitzgerald, S. G., Cooper, R., & Boninger, M. L. (2004). Impact of a pushrim-activated power-assisted wheelchair on the metabolic demands, stroke frequency, and range of motion among subjects with tetraplegia. Archives of Physical Medicine and Rehabilitation, 85(11), 1865-1871.

[9] Cooper, R. A., Corfman, T. A., Fitzgerald, S. G., Boninger, M. L., Spaeth, D. M., Ammer, W., & Arva, J. (2002). Performance assessment of a pushrim-activated power-assisted wheelchair control system. IEEE Transactions on control systems technology, 10(1), 121-126.

[10] Oonishi, Y., Oh, S., & Hori, Y. (2010). A new control method for power-assisted wheelchair based on the surface myoelectric signal. IEEE Transactions on Industrial Electronics, 57(9), 3191-3196.

[11] Oh, S., Hata, N., & Hori, Y. (2005, June). Control developments for wheelchairs in slope environments. In Proceedings of the 2005, American Control Conference, 2005. (pp. 739-744). IEEE.

[12] Ou, C. C., & Chen, T. C. (2012). Power-Assisted Wheelchair Design based on a Lyapunov Torque Observer. International Journal of Innovative Computing Information and Control, 8(12), 8089-8102.

[13] Shibata, T., & Murakami, T. (2008, March). Power assist control by repulsive compliance control of electric wheelchair. In 2008 10th IEEE International Workshop on Advanced Motion Control (pp. 504-509).

[14] Kim, D. Y., Kim, K. S., Kim, J. M., & Kim, J. M. (2016). Control Method of Power-Assist Device using a BLDC motor for Manual Wheelchair. JOURNAL OF POWER ELECTRONICS, 16(2), 798-804.

[15] Tsai, M. C., & Hsueh, P. W. (2012, July). Synchronized motion control for 2D joystick-based electric wheelchair driven by two wheel motors. In 2012 IEEE/ASME International Conference on Advanced Intelligent Mechatronics (AIM) (pp. 702-707). IEEE.

[16] Giesbrecht, E. M., Ripat, J. D., Quanbury, A. O., & Cooper, J. E. (2009). Participation in community-based activities of daily living: comparison of a pushrim-activated, power-assisted wheelchair and a power wheelchair. Disability and Rehabilitation: Assistive Technology, 4(3), 198-207.

[17] De La Cruz, C., Bastos, T. F., & Carelli, R. (2011). Adaptive motion control law of a robotic wheelchair. Control Engineering Practice, 19(2), 113-125.

[18] Giesbrecht, E. M., Ripat, J. D., Quanbury, A. O., & Cooper, J. E. (2009). Participation in community-based activities of daily living: comparison of a pushrim-activated, power-assisted wheelchair and a power wheelchair. Disability and Rehabilitation: Assistive Technology, 4(3), 198-207.

[19] Fay, B. T., & Boninger, M. L. (2002). The science behind mobility devices for individuals with multiple sclerosis. Medical engineering & physics, 24(6), 375-383.

[20] Mohammad, S., Guerra, T. M., Pudlo, P., "Method and device assisting with the electric propulsion of a rolling system, wheelchair kit comprising such a device and wheelchair equipped with such a device". Patent WO2015173094 A1, issued 19.11.2015.

[21] Estrada-Manzo, V., Lendek, Z., & Guerra, T. M. (2015, December). Unknown input estimation for nonlinear descriptor systems via LMIs and Takagi-Sugeno models. In 2015 54th IEEE Conference on Decision and Control (CDC) (pp. 6349-6354). IEEE.

[22] Estrada-Manzo, V., Lendek, Z., & Guerra, T. M. (2016). Generalized LMI observer design for discrete-time nonlinear descriptor models. Neurocomputing, 182, 210-220.

[23] Guerra, T. M., Estrada-Manzo, V., & Lendek, Z. (2015). Observer design for Takagi–Sugeno descriptor models: An LMI approach. Automatica, 52, 154-159.

[24] de Oliveira, M. C., & Skelton, R. E. (2001). Stability tests for constrained linear systems. In Perspectives in robust control (pp. 241-257). Springer London.

[25] Jiang, Z. P., & Wang, Y. (2001). Input-to-state stability for discrete-time nonlinear systems. Automatica, 37(6), 857-869.

[26] World Health Organization. (2011). World report on disability. World Health Organization.

[27] Ahn, Choon Ki, Peng Shi, and Michael V. Basin. "Deadbeat dissipative FIR filtering." IEEE Transactions on Circuits and Systems I: Regular Papers 63.8 (2016): 1210-1221.

[28] Zhang, Jiancheng, et al. "Robust impulsive reset observers of a class of switched nonlinear systems with unknown inputs." Journal of the Franklin Institute 354.7 (2017): 2924-2943.

[29] Guan, Yuping, and Mehrdad Saif. "A novel approach to the design of unknown input observers." IEEE Transactions on Automatic Control 36.5 (1991): 632-635.